

SUPPLEMENTAL MATERIAL

Contents:

- **SUPPLEMENTARY METHODS**
- **SUPPLEMENTARY FIGURES & FIGURE LEGENDS**
- **SUPPLEMENTARY TABLES & TABLE LEGENDS**

SUPPLEMENTARY METHODS

Human samples

Tumor samples at diagnosis and relapse from index case and five healthy thymus samples were obtained from Hospital Fundación Jiménez Díaz and Hospital La Paz, respectively. Human postnatal thymocytes were isolated from thymuses removed during cardiac surgery in pediatric patients. Institutional review board approval was obtained for this study (CEI-70-1260), and the participants provided written informed consent in accordance with the Declaration of Helsinki.

Index case

A 16-year-old boy diagnosed in 2019 with pre-T/cortical T-ALL (EGIL T-II/III), according to the European Group for the Immunological characterization of Leukaemias (EGIL) classification. The patient presented symptoms of asthenia, lumbar pain, nausea and diarrhoea. He had two left latero-cervical lymphadenopathies, a smaller retro-auricular mastoid lymphadenopathy and a left supraclavicular lymphadenopathy. The patient presented 92% of blasts at blood examination and smear test. He achieved complete remission upon treatment with the LAL/SEHOP-PETHEMA 2013 protocol (version 2.0, 10/09/2014) approved by the Spanish Society of Pediatric Hematology and Oncology (SEHOP) and the Program for the Study of Therapeutics in Hematological Malignancies protocol (PETHEMA). Specifically, the index case received a pre-phase stage corticosteroid treatment (prednisone) at admission, followed by two induction cycles (IA and IB) and one intensification cycle (block AR-1) consisting of: vincristine, daunorubicin, L-asparaginase, cyclophosphamide, 6-mercaptopurine, cytarabine, dexamethasone and methotrexate. Monitoring of minimal residual disease (MRD) gave values of 1.02% after induction cycle IA, <0.1% after induction cycle IB and <0.1% after intensification cycle. For CNS prophylaxis, triple intrathecal chemotherapy (methotrexate, cytarabine and hydrocortisone) was administered by lumbar puncture. He received an allogeneic hematopoietic stem cell transplant from a HLA-identical sister, after myelo-ablative conditioning with thiotepa, fludarabine and busulphan as well as graft versus host prophylaxis with postransplant cyclophosphamide and cyclosporin/mycophenolate. One year later the patient experienced a relapse and was treated with neralabine but the development of high liver toxicity led to treatment discontinuation and he eventually expired in January 2020. Tumor samples were obtained from peripheral blood at diagnosis and at relapse. The samples were treated with Ficoll and, in the case of relapse, sorted for blast population using the antibody panel described in **Supplementary Table S2** and a BD InFLux cell sorter (Becton Dickinson).

Cell lines

The JURKAT clone E6-1 (ATCC#TIB-152) and HEK-293T (ATCC Cat# CRL-11268, RRID:CVCL_1926) cells were purchased from ATCC. The BCR-ABL1 positive cell line K562 (DSMZ#ACC10), Ba/F3 (DSMZ#ACC300) and M07e (DSMZ# ACC104) cells were purchased from DSMZ.

Suspension cells were cultured in RPMI 1640 (Gibco, Life Technologies) supplemented with 10% fetal bovine serum (GE Healthcare Life Sciences), 2mM L-glutamine (Merck Millipore) and, in the case of JURKAT, 1mM sodium pyruvate (Merck Millipore). HEK-293T cells were cultured in Dulbecco's Modified Eagle's Medium supplemented with 10% fetal bovine serum, 2mM L-glutamine and 1mM sodium pyruvate.

Ba/F3 and M07e cells, which require cytokines or growth factors for normal viability and proliferation, were routinely cultured with 5 ng/ml of interleukin-3 (Cell Signaling Technology) or with 10 ng/ml granulocyte-monocyte colony-stimulating factor (R&D Systems) respectively. For experimental assays, cells were washed three times with 1X PBS and cultured in medium free of cytokines and growth factors.

Cell experimentation was always performed within a period not exceeding 6 months after resuscitation. Cultures were maintained in 5% CO₂ humidified atmosphere at 37°C. ATCC and DSMZ routinely perform cell lines authentication using STR analysis (DNA profiling) as a procedure.

Generation of stable cell lines

M07e and Ba/F3 cells were transduced with lentiviral particles carrying the SEPTIN6::ABL2 fusion, *ABL2*^{WT} or a stuffer (NEG) obtained after HEK-293T-mediated packaging using pMD2.G and psPAX2 (Addgene; RRID:Addgene_12260). Lentiviral vectors were purchased from VectorBuilder Inc. Transfection was accomplished using Lipofectamine2000 (Thermo Fisher Scientific, Inc.). To obtain cell populations with comparable expression, transduced cells were sorted for similar EGFP levels using FACS (FACSCVantage SE, BD Biosciences, RRID:SCR_013311).

Next generation sequencing

- Whole exome sequencing (WES)

Total DNA was isolated using a DNeasy 96 Blood and Tissue Kit (Qiagen) according to the manufacturer's instructions. DNA quantification and quality were checked by Nanodrop (Thermo Fisher Scientific Inc.), Qubit (Thermo Fisher Scientific Inc) and TapeStation (Agilent Technologies). Whole exome sequencing was performed by NIMGenetics SL using the Sure Select All Exome V6 system (Agilent Technologies). The libraries were generated with SureSelectXT Human All Exon V6 technology, from Covaris-fragmented genomic DNA (150-200 bp). From the amplified libraries, the genomic regions of interest were captured using 120 bp RNA probes (SureSelectXT). The generated libraries were normalized and combined into equimolecular concentrations for optimal generation of DNA clusters. Paired-end sequencing

(2x150 bp) of the SureSelectXT libraries, previously enriched, indexed and multiplexed, was carried out in the NovaSeq 6000 platform (Illumina, Inc). Sequencing data were demultiplexed using the bcl2fastq2 software (Illumina) and quality was assessed using the FASTQC tool (<https://www.bioinformatics.babraham.ac.uk/projects/fastqc/>). Alignment was performed using Burrows-Wheeler Aligner (BWA-MEM) against GRCh37/hg19 assembly. Results were recalibrated to improve local quality. All these tools are available in the GATK toolkit¹, and have been used following recommended Best Practices guide (<https://gatk.broadinstitute.org/hc/en-us/sections/360007226651-Best-Practices-Workflows>). Variant calling was performed using a combination of MuTect tool² and VarScan 2³. Variant annotation and effect prediction were performed with ANNOVAR tool⁴, including information from the Single Nucleotide Polymorphism Database (dbSNP, build 135), the 1000 Genomes Project, the Exome Variant Server (NHLBI GO Exome Sequencing Project, Seattle, WA, USA) and 'in-house' scripts.

- RNA sequencing (RNA-seq)

Total RNA was isolated using the miRNeasy Mini Kit (Qiagen) according to the manufacturer's instructions. RNA quantification and quality were checked by Nanodrop (Thermo Fisher Scientific Inc.), Qubit (Thermo Fisher Scientific Inc) and TapeStation (Agilent Technologies). RNA-seq was performed by NIMGenetics SL. Libraries preparation was performed using TruSeq Stranded Total RNA Library Prep (Illumina, Inc.) and included rRNA depletion, fragmentation, cDNA synthesis and adaptor ligation. The generated libraries were normalized and combined in equimolecular concentrations for optimal generation of DNA clusters. Paired-end sequencing (2x100bp) of the previously enriched, indexed and multiplexed libraries were performed on the high-throughput NovaSeq 6000 platform (Illumina Inc.), with a minimum of 100M PE reads (50+50) per sample, with a read quality of 85%>Q30. For bioinformatics analysis, GRCh38/hg38 (Ensembl version 103) genome was used as a reference. Briefly, quality check and sequence trimming were performed using the FASTQC tool and fastp⁵ respectively, then the trimmed RNA-seq reads were aligned against the reference genome. Following the alignment, the transcripts were assembled using HISAT2 tool⁶, corresponding genes were obtained and their expression abundance was determined using StringTie suite (<https://ccb.jhu.edu/software/stringtie/>). On gene counting matrices, reads were subjected to unsupervised filtering in order to discard those genes with very few or no reads throughout all the samples of the study (<https://bioconductor.org/packages/release/bioc/html/genefilter.html>). Genes with a total abundance below 15 total reads were excluded from further analysis.

- **Fusion transcript analysis**

From the raw (Fastq) RNA-seq data, gene fusions were studied using the FusionCatcher suite (<https://github.com/ndaniel/fusioncatcher>), and the results were analyzed to determine the

reliability of each fusion. After trimming and alignment of the sequences with different RNA-seq aligners (Bowtie⁷, Bowtie 2⁸, STAR⁹, BLAT¹⁰), the resulting fusions were filtered according to the number of replicates (minimum 2) and spurious coincidences were eliminated. Additional filters were applied, so that fusions with counts of common mapping reads above 0, with spanning pairs and spanning unique reads below 10 and/or with longest anchor found below 25 were filtered out; fusions identified solely by Bowtie were also considered false positives and subsequently filtered out. *SEPTIN6::ABL2* fusion breakpoint was confirmed in the primary tumor sample from index case at the genomic and transcript levels by Sanger DNA sequencing of PCR-amplified fusion sequence, using oligonucleotides described in **Supplementary Table S3**.

Structural and copy number variant analyses

- Comparative Genomic Hybridization Array (aCGH)

aCGH analyses were performed by NIMGenetics SL, using an Array-CGH+SNP Cytoscan HD-750k Affymetrix for diagnosis and relapse samples (manufactured by Agilent Technologies). The average resolution of the analysis was approximately 75kb for the syndromic regions of the design (40 kb for the critical genes included), and 100 kb for the rest of the genome. For bioinformatics analysis, the GRCh37/hg19 genome was used as a reference, and the ADM-2 statistic (0.5Mb window, A=6) was applied.

- Multiplex Ligation-dependent Probe Amplification (MLPA)

Multiplex ligation-dependent probe amplification (MLPA) was performed by NIMGenetics SL for copy-number analysis of *CDKN2A* using the Salsa ME024 (MRC-Holland) kit.

- Fluorescence *in situ* hybridization (FISH)

XL ABL2 BA Break Apart Probe and centromeric probes for chromosome 17 were purchased from Metasystems Probes.

Two sets of bacterial artificial chromosome (BAC) clones (RP11-379J1, RP11-207G22, RP11-142H10 and CH17-453G14 for *SEPTIN6*; and RP11-152K11, RP11-170H10, RP11-124A5 and RP11-1054P1 for *ABL2*) were obtained from the BACPAC Resources Centre (<https://bacpacresources.org/>) to generate a two-color dual-fusion FISH probe to detect chromosome translocation resulting in *SEPTIN6::ABL2* fusion. *SEPTIN6* BACs were labeled with Spectrum-Orange, and *ABL2* BACs with Spectrum-Green.

FISH analyses were performed as previously published¹¹. Briefly, cells exposed to colcemid to arrest mitosis at the metaphase stage were treated with a hypotonic solution and fixed with glacial acetic acid and methanol. After dehydration, the samples were denatured in the presence of the specific probe at 73°C and incubated overnight for hybridization at 37°C. Finally, the slides were washed in 20SSC (saline-sodium citrate) buffer with detergent Tween-20 and mounted on fluorescent mounting media (DAPI in antifade solution).

For *ABL2* and chromosome 17 FISH, a NIKON eclipse 80i fluorescence microscope with a 100x oil-immersion objective, NIKON DAPI, green, and orange fluorescence filter cubes, and Cool Cube 1 CCD camera (Metasystems, Germany) connected to a PC running the ISIS fluorescence imaging platform image analysis system (Metasystems) with Z stack software was used to image 200 cells.

For *SEPTIN6::ABL2* FISH, a Leica DM 5500B fluorescence microscope with a 100x oil-immersion objective, Leica DM DAPI, green, and orange fluorescence filter cubes, and a CCD camera (Photometrics SenSys camera) connected to a PC running the Zytovision image analysis system (Applied Imaging Ltd., UK) with Z stack software was used to image 200 cells. The z-stack images were manually scored by two independent investigators by counting the number of co-localized signals, representing fused transcripts.

Western-Blot (WB)

Total protein extracts obtained using RIPA lysis buffer (50mM Tris-HCl pH 7.4, 150mM NaCl, 1% triton X-100, 0.5% Deoxycholate and 0.1% SDS). Then, proteins extracts were supplemented with 2mM phenylmethylsulphonyl fluoride, 2.5µl/ml Protease Inhibitor Cocktail and 10µl/ml Phosphatase Inhibitor Cocktail 2 (Roche Diagnostics GmbH) as previously described¹². Ten-microgram aliquots of total protein extracts were electrophoresed in 30% acrylamide/bis-acrylamide solution 29:1 (Bio-Rad Laboratories, RRID:SCR_008426) and then electro-transferred to mini-sized nitrocellulose membranes using the Transfer Blot® Turbo™ Transfer System (Bio-Rad Laboratories). Peroxidase activity was detected using a WesternBright ECL Detection System (Advansta). Secondary antibodies were conjugated to horseradish peroxidase (GE Healthcare Life Sciences), and the bands were visualized using a cooled charge-coupled device camera (ImageQuant LAS-4000; GE Healthcare Life Sciences).

Antibodies and reagents

The antibodies used for immunodetection are summarized in **Supplementary Table S2**. Tyrosine kinase inhibitors were purchased from Selleckchem and used within the dose range recommended by manufacturers: imatinib (#STI571; 0.1, 0.5 or 1µM), nilotinib (#AMN-107; 10, 50 or 100nM) and dasatinib (#BMS-354825; 1, 5 or 10nM). In functional assays involving pharmacological inhibitors, cells were cultured in parallel with equivalent amounts of dimethyl sulfoxide (DMSO) as a vehicle control.

***SEPTIN6::ABL2* fusion cDNA cloning**

Reverse transcription from total RNA of Patient_Rx was performed using the SuperScript™ VILO™ cDNA Synthesis Kit (Invitrogen), followed by PCR with the Expand High Fidelity PCR System (Roche), as indicated by the manufacturers. Primer sequences are listed in **Supplementary Table S3**, and the annealing temperature was 60 °C. PCR products were purified

using the Wizard SV Gel and PCR Clean-up System (Promega Corporation) and cloned into the pGEM-T-Easy vector system (Promega; RRID:Addgene_25782). Subsequently, the *SEPTIN6::ABL2* fusion cDNA was subcloned into a mammalian gene expression lentiviral vector carrying the EF1A promoter to drive *SEPTIN6::ABL2* expression and EGFP marker for monitoring. The presence and intact sequence of the *SEPTIN6::ABL2* fusion cDNA was checked by Sanger sequencing in both pGEM-T-Easy and lentiviral clones, using the oligonucleotides described in **Supplementary Table S3**.

Reverse transcription quantitative polymerase chain reaction (RT-qPCR)

Gene expression was determined by real-time quantitative RT-PCR from total RNA in two steps using the High-Capacity RNA-to-cDNA™ Kit for retro-transcription (RT) and the Fast SYBR® Green Master Mix kit for qPCR in ABI PRISM 7900HT SDS (all from Applied Biosystems). Expression values of the housekeeping genes *ACTB* and *B2M* in the same samples were used for normalization using the $2^{-\Delta\Delta CT}$ method¹³. The oligonucleotide sequences are shown in **Supplementary Table S3**.

Trypan blue exclusion analysis

To analyze cell growth, viable cells were counted using trypan blue exclusion and the TC10 Automated Cell Counter (Bio-Rad Laboratories). When required, the cells were washed, seeded at 500.000 cells/ml and treated with vehicle or the appropriate inhibitor for 72h for Ba/F3, K562 and Jurkat.

Flow Cytometry

Flow cytometry experiments were performed using a FACS Canto A cytometer (BD Biosciences), and the results were analyzed using FlowJo v10 (LLC), RRID:SCR_008520. Cell cycle was profiled using PI/RNase Staining Buffer (BD Biosciences). When indicated, cells were washed, seeded at 500.000 cells/ml and treated with vehicle or the appropriate inhibitor during 24h for K562, Jurkat and Ba/F3 cells transduced with *SEPTIN6::ABL2* (Ba/F3-SA). Watson pragmatic fitting algorithm was used to determine cell cycle phase statistics using FlowJo v10. Viability was monitored using the PE Annexin-V Apoptosis Detection Kit I (BD Biosciences). Where indicated, cells were washed, seeded at 500.000 cels/ml and treated with vehicle or the appropriate inhibitor during 72h for K562, Jurkat and Ba/F3-SA.

Statistical analysis

Normality tests were performed using “Shapiro-Wilk test”. Unpaired two tailed t-test was used for qPCR analysis and for the rest multiple comparisons were conducted using one- and two-way analysis of variance (ANOVA). To avoid potential issues derived from multiple testing, appropriate statistical corrections have been applied using “Dunnett's multiple comparisons test” or “Sidak's multiple comparisons test”. Statistical significance was set at $P < 0.05$. Statistical

analyses were performed using the GraphPad Prism, RRID:SCR_002798, version 8. Detailed information about statistical analyses is summarized in Supplementary Table S4.

Supplementary Fig. S1. Genomic characteristics of index case. (A) List of mutations in the patient. Mutations in prominent known ALL oncogenes and tumor suppressors were selected when affecting a canonical isoform (according to APPRIS) and eliciting a pathogenic prediction both by PolyPhen and SIFT algorithms. Saliva DNA was used to discriminate between somatic and germline mutations. (B) Comparative genomic hybridization array (aCGH) of patient tumor sample at diagnosis (Patient Dx, top) and relapse (Patient Rx, bottom). (C) Trisomy of chromosome 17 in Patient Dx (left) and Patient Rx (right) observed by FISH analysis of interphase cells using a centromeric chromosome 17 (CEP17) probe. FISH images are representative examples of at least three independent experiments. (D) Patient Dx (left) and Patient Rx (right) exhibit a homozygous loss of *CDKN2A* affecting exons 2 to 5 and flanking regions, as determined by Multiplex Ligation-dependent Probe Amplification (MLPA).

Supplementary Fig. S2.

***SEPTIN6::ABL2* cDNA**

ATG GCAGCGACCGATATAGCTCGCCAGGTGGGTGAAGGTTGCCGAAGTGTCCCCCTGGCTGGACATGTGGGGTTTGACAGCTTGCCT
GACCAGCTGGTGAATAAGTCCGTCAGCCAGGGCTTCTGCTTCAACATCCTGTGCGTGGGAGAGACAGGTTTGGGCAAGTCCACCCTC
ATGGACACCCTGTTCAACACCAAATTCGAAGGGGAGCCAGCCACCCACACACAGCCGGGTGTCCAGCTCCAGTCTAATACCTATGAC
CTCCAAGAGAGCAACGTGAGGCTAAAGCTCAGCATCGTTAGCACAGTTGGCTTTGGGGACCAGATCAACAAAGAGGACAGCTACAAG
CCTATCGTGGAATTCATCGATGCACAATTCGAGGCCTACCTGCAGGAAGAGCTAAAGATCCGAAGAGTGCTACACACCTACCATGACT
CCCGAATCCATGTCTGCTTGTATTTTCATTGCCCCACGGGTTCATTCCCTGAAGTCTCTGGACCTAGTGACTATGAAGAAGCTGGACAGT
AAGGTGAACATCATCCCCATCATTGCCAAAGCAGATGCCATTTGGAAGAGTGAGCTAACAAAGTTCAAATCAAATCACCAGCGAGCT
TGTCAGCAACGGAGTCCAGATCTATCAGTTTCTACAGATGATGAGTCGGTGGCAGAGATCAATGGAACCATGAACGCCACCTGCCG
TTTGCTGTCAATGGCAGCACAGAAGAACTGAAGATAGGCAACAAGATGATGAGGGCGCGGCAGTATCCTTGGGGCACTGTGCAGGTT
GAAAACGAGGCCCACTGCGACTTTGTGAAGCTGCGGGAGATGCTGATTGCGGTCAACATGGAGGATCTGCGGGAGCAGACCCACAC
CCGGCACTATGAGCTGTATCGCCGCTGTAAGCTGGAGGAGATGGGCTTCAAGGACACCGACCCTGACAGCAAACCCTTCAAGTTTACA
GGAGACATATGAGGCCAAAAGGAACGAGTTCCTAGGGGAAGTCCAGAAAAAAGAAGAGGAGATGAGACAGATGTTTCGTCAGCGAGT
CAAAGAGAAAAGAAGCGGAGCTCAAAGAGGCAGAGAAAAGAGTGTATGTGACTGCTGAGAGCCGCTTCAGCACCTGGCAGAGCTT
GTACA CCATCCATCCACAGTGGCTGATGGGCTGGTGACAACATTACACTACCCAGCACCCCAAGTGTAATAAGCCTACAGTCTATGGT
TGTCCTCCATCCACGACAAATGGGAAATGGAGCGAACAGATATTACCATGAAGCACAAACTTGGGGCGGTGAGTATGGAGAGGTTTA
CGTTGGCGTCTGGAAGAAATACAGCCTTACAGTTGCTGTGAAAACATTGAAGGAAGATACCATGGAGGTAGAAGAATTCCTGAAAGAA
GCTGCAGTAATGAAGGAAATCAAGCATCCTAATCTGGTACAACTTTTAGGTGTGTGACTTTGGAGCCACCATTTTACATTGTGACTGAA
TACATGCCATACGGGAATTTGCTGGATTACCTCCGAGAATGCAACCCGAGAAGAGGTGACTGCAGTTGTGCTGCTCTACATGGCCACTC
AGATTTCTTCTGCAATGGAGTACTTAGAGAAGAAGAATTTTATCCATAGAGATCTTGCAGCTCGTAACTGCCTAGTGGGAGAAAACCAT
GTGGTAAAAGTGGCTGACTTTGGCTTAAGTAGATTGATGACTGGAGACACTTATACTGCTCATGCTGGAGCCAAATTTCTATTAAGTG
GACAGCACCAGAGAGTCTTGCCTACAATACCTTCTCAATTAATCTGACGCTCTGGGCTTTTGGGGTATTGTTGTGGGAAATGCTACCT
ATGGAATGTCCATATCCAGGTATTGACCTGTCTCAGTCTATGACCTACTAGAAAAAGGATATCGAATGGAACAGCCTGAGGGATG
CCCCCTAAGGTTTATGAACCTTATGAGAGCATGCTGGAAGTGGAGCCCTGCCGATAGGCCCTCTTTGTGAAACACACCAAGCTTTT
GAAACCATGTTCCATGACTCCAGCATTCTGAAGAGGTAGCTGAGGAGCTTGGGAGAGCCGCCTCCTCGTATCTGTTGTTCCATACC
TGCCCCGGCTACCTATACTTCCCTTCAAGACTCGGACACTGAAGAAACAGGTGGAGAACAAGGAGAACATTGAAGGGGCACAAGATG
CCACAGAAAATCTGCTTCCAGTTTAGCACCAGGGTTTCATCAGAGGTGCACAGGCCTCTAGTGGATCCCCAGCACTGCCTCGAAAGCA
AAGAGACAAGTCAACCCAGCAGCCTCTTGGAAAGATGCCAAAGAGACATGCTTACCAGGGATAGGAAGGGGGGCTTCTTCACTCCTT
CATGAAGAAGAGAAATGCTCCTACACCCCCCAAACGCAGCAGCTCCTTCCGAGAAATGGAGAATCAGCCCCATAAGAAATACGAACTC
ACGGGTAACCTCTCATCTGTTGCTTCTCTACAGCATGCTGATGGGTTCTCTTCACTCCTGCCAGCAAGAGGCGAATCTGGTGCCAC
CCAAGTGCTATGGGGGGAGCTTTGCACAGAGGAACCTCTGTAATGACGACGGTGGTGGGGGTGGGGGCAGTGGCACTGCTGGGGGT
GGGTGGCTGGCATCACAGGCTTCTTTACACCACGTTAATCAAAAAGACACTGGGCTTACGAGCAGGTAACCCACAGCCAGTGTATG
ACATTTCCAAGCCTTTTCCAAGGTCAAACCTACATCTTCCATGCTCCTCAGGGCTTCCAGAGCAGGATAGGATGGCAATGACCCCTCC
AGGAAGTCCAGAGGTCCAAACTCCAGCTGGAAGGACAGTGTCCACCTCTTCTCAGCCAGAAGAGAATGTGGACAGGGCCAATGAC
ATGCTTCCAAAAAATCAGAGGAAAGTGTGCTGCTCCAAGCAGGGAGAGACAAAAGCCAAGTTATTGCCAGAGGAGCCACAGCTCTTC
CTCTCAGAACACCCTCTGGGGATCTAGCCATTACAGAGAAGGACCCCTCAGGGGTGGGAGTGGCTGGAGTGGCACTGCCCCCAAG
GGTAAAGAGAAGATGTTGGGACAGACTTGGGATGGCTGGATTCAGGATGGAGAGCAGCCGGCTGGCCTTCCAGCCAA
GGCTGCCCCCGTCTCCTCAACCACTCACAACCACAAAGTGCCAGTCTTATCTCACCCTCTGAAACACACTCCAGCTGACGTGCAG
CTCATTGGCACAGACTCTCAGGGGAATAAATCAAGCTCTTATCTGAGCATCAGGTCACATCCTCTGGAGACAAGGACCGACCCCGAC
GGGTAACCAAGTGTGCCCCACCCACCACAGTGTGAGACTACTGCAGCATCCGTCCATCTGCTCAGACCCCTACAGAAGAGC
CAACTGCCCTAACTGCAGGACAGTCCACATCAGAAAACAGGAAGGAGGAAAGAAGGCAGCTCTGGGCGCAGTGCCCATCAGTGGG
AAAGCTGGGAGGCCAGTGTGCTCCACCTCAAGTGCCTGCCCCACATCTCCATCTCGCCAGCCAAAATGGCCAATGGCACAGCA
GGTACTAAAGTGGCTCTGAGAAAACCAAACAGGCCGCTGAGAAAATCTCAGCAGACAAAATCAGCAAAGAGGGCCCTGCTGGAATGTG
CTGACCTACTGTCCAGTGCCTCAGGAACCTGTGCCAACAGCCAGCTGGTAGACTGGACACCAGCTGCTTGACTACTGCTCAG
GCTATGTGGACTGCATCCCTCAAACCTCGCAACAAATTTGCCTTCCGAGAGGCTGTGAGCAAACCTGGAAGTCAAGCTGCAGGAGCTACA
GGTTTCTCAGCAGCTGCTGGTGTGCCCGGACAAACCCTGTCTTAATAACTATTGTGCATGTGTACAGGAAATCAGTGTGTGGTGC
AGAGGTAG

Fusion breakpoint cDNA:

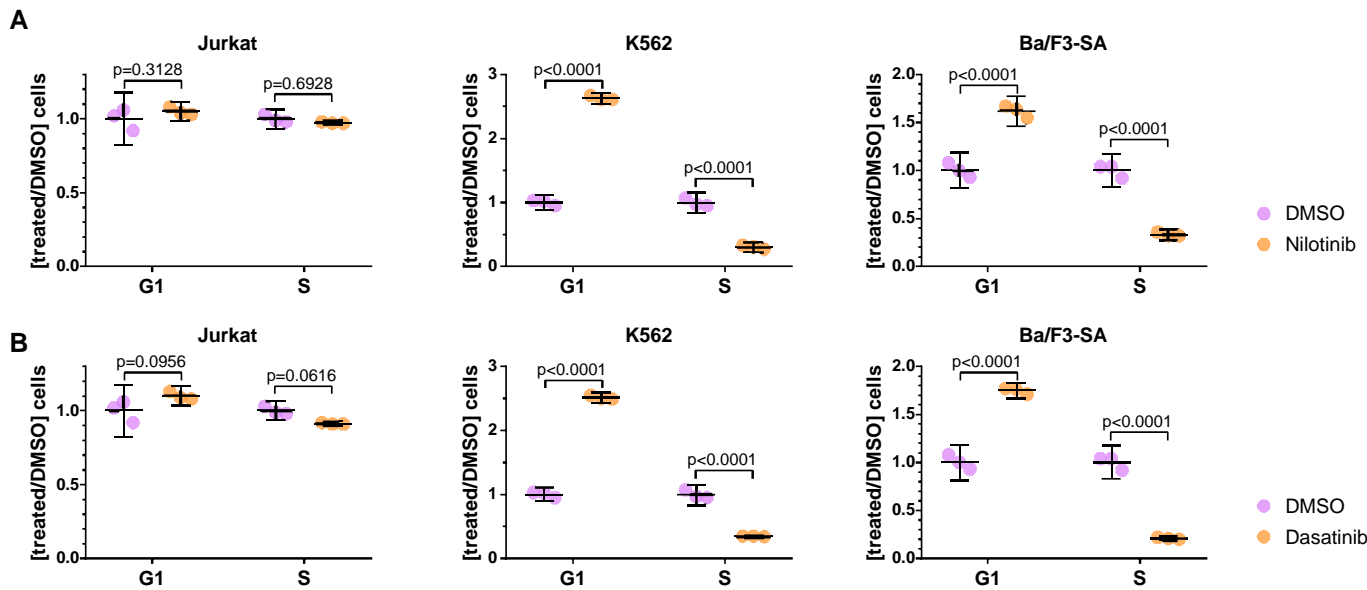
TCCAGCGAGTCAAAGAGAAAAGAAGCGGAGCTCAAAGAGGCAGAGAAAAGAGTGTATGTGACTGCTGAGAGCCGCTTCAGCACCTTGCAGAGCTTGTACA

SEPTIN6

ABL2

Supplementary Fig. S2. Identification of the novel *SEPTIN6::ABL2* fusion. Complete cDNA sequence of *SEPTIN6::ABL2* fusion. It is marked the fusion breakpoint in cDNA between *SEPTIN6* (yellow) and *ABL2* (blue).

Supplementary Fig. S3



Supplementary Fig. S3. Cell cycle analysis. (A) Cell cycle analysis of Jurkat (left), K562 (middle) and Ba/F3-SA (right) cells treated with Nilotinib (50nM) and referred to DMSO-treated cells. (B) Cell cycle analysis of Jurkat (left), K562 (middle) and Ba/F3-SA (right) cells treated with Dasatinib (5nM) and referred to DMSO-treated cells. The graphics in (A, B) show the mean with 95% confidence interval after three independent experiments. Multiple comparisons were made in (A, B) with respect to DMSO-treated cells. Statistical significance was set at $P < 0.05$.

SUPPLEMENTARY TABLES & TABLE LEGENDS

Supplementary Table S1. List of transcript fusions in index case.

From RNA-seq data in index case, gene fusions are analyzed. The criteria to identify reliable fusions were as follows:

- 1) Counts_of_common_mapping_reads: a number above 0 indicates that there are reads that align in both genes at the same time indicating high homology.
- 2) Spanning_pairs and Spanning_unique_reads: summarize the total reads that define the fusion. A very low number may imply that the finding is by chance.
- 3) Fusion_finding_method: indicates how many aligners support a fusion. If only one (usually bowtie) finds reads for a fusion, it will be considered as an indicator of false positive.
- 4) Longest_anchor_found: indicates the maximum length found in the anchor reads. A length less than 25 is considered anomalous and may indicate a false positive.
- 5) Fusion_description: annotation from different databases. Several are indicative of false positives and false fusions or have been found in healthy populations, occur between gene clones, between pseudogenes, genes are very close in the genome, etc. Special attention has been paid to those annotations related with cancer and oncogenes.
- 6) Repetition of fusions: in some cases, there are several fusions that present the same genes. This is because several of these genes may be very close together (usually clones), overlapping in the genome. Normally these genes encode for the same component.

		,exon- exon					BOWTIE +STAR							*GTGTATGTGACTGCTGAGAGC CGCTTCAGCACCTTGGCAGAGC	
SEPT6	ABL2	oncogen e,cancer ,exon- exon	0	259	44	46	BOWTIE ;BOWTI E+BLAT; BOWTIE +STAR	X:118767323:-	1:179091002:-	ENSG000001 25354	ENSG000001 43322	ENSE0000 1649048	ENSE0000 3676561	TCCAGCGAGTCAAAGAGAAAG AAGCGGAGCTCAAAGAGGCA GAGAAAGAG*GTGTATGTGAC TGCTGAGAGCCGCTTCAGCAC CTTGGCAGAGCTTGACA	in-frame

Supplementary Table S2. Antibodies.

List of antibodies used for Flow Cytometry and Western Blot in this study.

Antibodies for Flow Cytometry	Fluorochrome	Clone	Company
CD4	PE	13B8.2	Beckman Coulter
CD8	FITC	DK25	MilliporeSigma
CD5	PerCP-Cy5.5	L17F12	Becton Dickinson
CD56	PC7	N901/NKH	Beckman Coulter
CD7	APC	HIT7	Immunostep
CD3	APC-H7	SK7	Becton Dickinson
CD2	V-450	S5.2	Becton Dickinson
CD45	V-500	2D1	Becton Dickinson
Antibodies for Western Blot	Dilution	Species	Company, catalog no.
ABL2 [EPR1222(2)]	1/1000	Rabbit	Abcam, ab134134
c-ABL	1/1000	Rabbit	Cell Signaling, 2862
β-Actin (AC-15)	1/20000	Mouse	Sigma Aldrich, A5441
Phospho-tyrosine (4G10)	1/500	Mouse	Sigma Aldrich, 05-321
anti-mouse IgG HRP-linked antibody	1/1000	-	Cell Signaling, 7076
anti-rabbit IgG HRP-linked antibody	1/1000	-	Cell Signaling, 7074

Supplementary Table S3. Oligonucleotides.

List of oligonucleotides used in this study, indicating the application and sequence (5' to 3').

Application	Name	Sequence (5' > 3')
<i>SEPTIN6::ABL2</i> fusion full cDNA amplification	SA_cDNA_Fw	GAGCGATGGCAGCGACCGATA
	SA_cDNA_Rv	TCCCTCTCCCCTCAGAAATGTGTGCA
Sanger sequencing of <i>SEPTIN6::ABL2</i> fusion breakpoint and qPCR	SA_fb_Fw	TATGAGGCCAAAAGGAACGA
	SA_fb_Rv	GGGGGACACACCATAGACTG
Sanger sequencing of <i>SEPTIN6::ABL2</i> fusion	SA_Seq 1_Fw	GTTTCCTGTGCAGTAGCTCC
	SA_Seq 1_Rv	TCTTCTGTGCTGCCAATGAC
	SA_Seq 2_Fw	GATGAGTCGGTGGCAGAGAT
	SA_Seq 2_Rv	CTCCATTTCCCATTTGTCGT
	SA_Seq 3_Fw	TTGGCAGAGCTTGTACACCA
	SA_Seq 3_Rv	CCACATGGTTTTCTCCCACT
	SA_Seq 4_Fw	CTGCTTACATGGCCACTCA
	SA_Seq 4_Rv	ACCTCTGATGAACCCTGGTG
	SA_Seq 5_Fw	GCACAAGATGCCACAGAAAA
	SA_Seq 5_Rv	CTGGCTGAGAAGAGGTGGAC
	SA_Seq 6_Fw	TAGGATGGCAATGACCCTTC
	SA_Seq 6_Rv	GAGCTGCCTTCTTTCCTCT
	SA_Seq 7_Fw	CACAACCACAAAGTGCCAGT
	SA_Seq 7_Rv	GATTCCTGTACACATGACAATAAG
qPCR	<i>ACTB</i> _Fw	AGTGTGACGTGGACATCCGCAAAG
	<i>ACTB</i> _Rv	ATCCACATCTGCTGGAAGGTGGAC
	<i>B2M</i> _Fw	CCAGCAGAGAATGGAAAGTC
	<i>B2M</i> _Rv	GATGCTGCTTACATGTCTCG
	<i>SEPTIN6::ABL2</i> _Fw	TATGAGGCCAAAAGGAACGA
	<i>SEPTIN6::ABL2</i> _Rv	GGGGGACACACCATAGACTG

Supplementary Table S4. Statistical analyses

Details on statistical analyses are displayed for each figure, including the tests performed in each case, the mean and standard deviation (s.d.) of each condition, the effect size as a difference of the means, the confidence intervals (CI) of the difference at 95% and the corresponding P values or adjusted P values.

Figure 1E	Unpaired t test, Two-tailed						
	Mean CTRL	Mean Patient Rx	s.d. CTRL	s.d. Patient Rx	Mean Difference	95% CI of difference	P Value
	1	109.8	0.6151	8.9940	108.8	94.39 to 123.3	<0.0001
Figure 2A top	One-way ANOVA; Dunnett's multiple comparisons test						
	Mean A	Mean B	s.d. A	s.d. B	Mean Difference	95% CI of difference	Adjusted P Value
NEG (A) vs <i>ABL2</i> ^{WT} (B)	0.455	0.3827	0.0433	0.0175	0.07233	-0.0008433 to 0.1455	0.0522
NEG (A) vs <i>SEPTIN6::ABL2</i> (B)	0.455	1.128	0.0433	0.0275	-0.6733	-0.7465 to -0.6002	<0.0001
Figure 2A bottom	One-way ANOVA; Dunnett's multiple comparisons test						
	Mean A	Mean B	s.d. A	s.d. B	Mean Difference	95% CI of difference	Adjusted P Value
NEG (A) vs <i>ABL2</i> ^{WT} (B)	50.07	57.35	3.9580	2.8020	-7.276	-16.53 to 1.983	0.1116
NEG (A) vs <i>SEPTIN6::ABL2</i> (B)	50.07	69.16	3.9580	4.8520	-19.09	-28.34 to -9.826	0.0019
Figure 2C top	One-way ANOVA; Dunnett's multiple comparisons test						
	Mean A	Mean B	s.d. A	s.d. B	Mean Difference	95% CI of difference	Adjusted P Value
NEG (A) vs <i>ABL2</i> ^{WT} (B)	0.08667	0.1	0.0202	0.0557	-0.01333	-0.2456 to 0.2189	0.9805
NEG (A) vs <i>SEPTIN6::ABL2</i> (B)	0.08667	2.462	0.0202	0.1616	-2.375	-2.607 to -2.143	<0.0001
Figure 2C bottom	One-way ANOVA; Dunnett's multiple comparisons test						
	Mean A	Mean B	s.d. A	s.d. B	Mean Difference	95% CI of difference	Adjusted P Value
NEG (A) vs <i>ABL2</i> ^{WT} (B)	22.12	24.31	2.9430	10.6600	-2.185	-17.23 to 12.86	0.8847
NEG (A) vs <i>SEPTIN6::ABL2</i> (B)	22.12	86.5	2.9430	1.3600	-64.38	-79.42 to -49.33	<0.0001

Figure 2E top	Two-way ANOVA; Dunnett's multiple comparisons test						
	Mean 1	Mean 2	s.d. 1	s.d. 2	Mean Difference	95% CI of difference	Adjusted P Value
Jurkat							
0 vs. 0.1	1.0	0.9344	0.1913	0.1886	0.06564	-0.1828 to 0.3141	0.8455
0 vs. 0.5	1.0	0.9544	0.1913	0.2206	0.04556	-0.2029 to 0.2940	0.9388
0 vs. 1	1.0	0.99	0.1913	0.0841	0.01004	-0.2384 to 0.2585	0.9992
K562	1.0						
0 vs. 0.1	1.0	0.9235	0.0229	0.1562	0.07652	-0.1726 to 0.3257	0.7867
0 vs. 0.5	1.0	0.3536	0.0229	0.0812	0.6464	0.3973 to 0.8956	<0.0001
0 vs. 1	1.0	0.2612	0.0229	0.0672	0.7388	0.4602 to 1.017	<0.0001
Ba/F3-SA							
0 vs. 0.1	1.0	0.7857	0.0045	0.0809	0.2143	-0.03412 to 0.4627	0.101
0 vs. 0.5	1.0	0.1981	0.0045	0.0121	0.8019	0.5535 to 1.050	<0.0001
0 vs. 1	1.0	0.07536	0.0045	0.0069	0.9246	0.6762 to 1.173	<0.0001
Figure 2E middle	Two-way ANOVA; Dunnett's multiple comparisons test						
	Mean 1	Mean 2	s.d. 1	s.d. 2	Mean Difference	95% CI of difference	Adjusted P Value
Jurkat							
0 vs. 10	1.0	0.8154	0.1913	0.0623	0.1846	-0.07304 to 0.4422	0.2005
0 vs. 50	1.0	0.8973	0.1913	0.1407	0.1027	-0.1549 to 0.3603	0.6317
0 vs. 100	1.0	1.12	0.1913	0.3409	-0.1197	-0.3773 to 0.1379	0.5215
K562	1.0						
0 vs. 10	1.0	1.045	0.0229	0.0834	-0.04485	-0.3025 to 0.2127	0.9472
0 vs. 50	1.0	0.2612	0.0229	0.0079	0.7388	0.4812 to 0.9964	<0.0001
0 vs. 100	1.0	0.2084	0.0229	0.0254	0.7916	0.5340 to 1.049	<0.0001
Ba/F3-SA							
0 vs. 10	1.0	0.8169	0.0045	0.0688	0.1831	-0.07445 to 0.4407	0.2054

0 vs. 50	1.0	0.1634	0.0045	0.0209	0.8366	0.5790 to 1.094	<0.0001
0 vs. 100	1.0	0.1113	0.0045	0.0152	0.8887	0.6311 to 1.146	<0.0001
Figure 2E bottom	Two-way ANOVA; Dunnett's multiple comparisons test						
	Mean 1	Mean 2	s.d. 1	s.d. 2	Mean Difference	95% CI of difference	Adjusted P Value
Jurkat							
0 vs. 1	1.0	1.107	0.1913	0.2247	-0.1073	-0.3977 to 0.1830	0.6809
0 vs. 5	1.0	0.9328	0.1913	0.2560	0.06718	-0.2232 to 0.3575	0.8891
0 vs. 10	1.0	0.8973	0.1913	0.2068	0.1027	-0.1877 to 0.3931	0.7077
K562	1.0						
0 vs. 1	1.0	0.8417	0.0229	0.1990	0.1583	-0.1320 to 0.4487	0.3978
0 vs. 5	1.0	0.248	0.0229	0.0748	0.752	0.4616 to 1.042	<0.0001
0 vs. 10	1.0	0.1873	0.0229	0.0046	0.8127	0.5223 to 1.103	<0.0001
Ba/F3-SA							
0 vs. 1	1.0	0.5119	0.0045	0.0134	0.4881	0.1977 to 0.7784	0.0009
0 vs. 5	1.0	0.0655	0.0045	0.0064	0.9345	0.6441 to 1.225	<0.0001
0 vs. 10	1.0	0.04865	0.0045	0.0110	0.9514	0.6610 to 1.242	<0.0001
Figure 2F and Supplementary Figure S3	Two-way ANOVA; Sidak's multiple comparisons test						
	Mean DMSO	Mean Imatinib	s.d. DMSO	s.d. Imatinib	Mean Difference	95% CI of difference	Adjusted P Value
G1 phase							
DMSO vs Imatinib							
Jurkat	1.0	1.067	0.0696	0.0343	-0.06667	-0.1685 to 0.03516	0.2083
K562	1.0	2.497	0.0429	0.0272	-1.497	-1.589 to -1.405	<0.0001
Ba/F3-SA	1.0	1.623	0.0747	0.0662	-0.62	-0.7562 to -0.4838	<0.0001
S phase							
DMSO vs Imatinib							

Jurkat	1.0	0.9833	0.0265	0.0353	0.01667	-0.08516 to 0.1185	0.888
K562	1.0	0.42	0.0649	0.0103	0.5767	0.4845 to 0.6688	<0.0001
Ba/F3-SA	1.0	0.3667	0.0692	0.0195	0.6333	0.4971 to 0.7696	<0.0001
	Two-way ANOVA; Sidak's multiple comparisons test						
	Mean DMSO	Mean Nilotinib	s.d. DMSO	s.d. Nilotinib	Mean Difference	95% CI of difference	Adjusted P Value
G1 phase							
DMSO vs Nilotinib							
Jurkat	1.0	1.05	0.0696	0.0240	-0.05	-0.1412 to 0.04121	0.3128
K562	1.0	2.63	0.0429	0.0343	-1.63	-1.731 to -1.529	<0.0001
Ba/F3-SA	1.0	1.62	0.0747	0.0658	-0.6167	-0.7532 to -0.4801	<0.0001
S phase							
DMSO vs Nilotinib							
Jurkat	1.0	0.9733	0.0265	0.0064	0.02667	-0.06455 to 0.1179	0.6928
K562	1.0	0.3033	0.0649	0.0312	0.6933	0.5921 to 0.7945	<0.0001
Ba/F3-SA	1.0	0.3333	0.0692	0.0229	0.6667	0.5301 to 0.8032	<0.0001
	Two-way ANOVA; Sidak's multiple comparisons test						
	Mean DMSO	Mean Dasatinib	s.d. DMSO	s.d. Dasatinib	Mean Difference	95% CI of difference	Adjusted P Value
G1 phase							
DMSO vs Dasatinib							
Jurkat	1.0	1.1	0.0696	0.0273	-0.1	-0.2150 to 0.01497	0.0956
K562	1.0	2.513	0.0429	0.0315	-1.513	-1.608 to -1.419	<0.0001
Ba/F3-SA	1.0	1.747	0.0747	0.0333	-0.7433	-0.8638 to -0.6229	<0.0001
S phase							
DMSO vs Dasatinib							
Jurkat	1.0	0.9133	0.0265	0.0082	0.08667	-0.004547 to 0.1779	0.0616

K562	1.0	0.3467	0.0649	0.0076	0.65	0.5556 to 0.7444	<0.0001
Ba/F3-SA	1.0	0.21	0.0692	0.0118	0.79	0.6696 to 0.9104	<0.0001
Figure 2H left	Two-way ANOVA; Sidak's multiple comparisons test						
	Mean DMSO	Mean Imatinib	s.d. DMSO	s.d. Imatinib	Mean Difference	95% CI of difference	Adjusted P Value
DMSO vs Imatinib							
Jurkat	29.53	31.21	2.1917	4.3412	-1.677	-8.366 to 5.012	0.8755
K562	23.2	64.47	1.6203	3.9323	-41.26	-47.95 to -34.57	<0.0001
Ba/F3-SA	22.2	85.54	2.2438	2.3871	-63.39	-70.08 to -56.70	<0.0001
Figure 2H middle	Two-way ANOVA; Sidak's multiple comparisons test						
	Mean DMSO	Mean Nilotinib	s.d. DMSO	s.d. Nilotinib	Mean Difference	95% CI of difference	Adjusted P Value
DMSO vs Nilotinib							
Jurkat	29.53	29.41	2.1917	1.9354	0.1267	-4.028 to 4.281	0.9997
K562	23.2	70.43	1.6203	1.7786	-47.23	-51.38 to -43.08	<0.0001
Ba/F3-SA	22.2	81.93	2.2438	0.9304	-59.78	-63.93 to -55.63	<0.0001
Figure 2H right	Two-way ANOVA; Sidak's multiple comparisons test						
	Mean DMSO	Mean Dasatinib	s.d. DMSO	s.d. Dasatinib	Mean Difference	95% CI of difference	Adjusted P Value
DMSO vs Dasatinib							
Jurkat	29.5	36.56	2.1917	3.3963	-7.023	-16.20 to 2.155	0.1576
K562	23.2	64.37	1.6203	8.5851	-41.16	-50.34 to -31.98	<0.0001
Ba/F3-SA	22.2	94.97	2.2438	1.0436	-72.82	-82.00 to -63.64	<0.0001

SUPPLEMENTARY REFERENCES

1. Van der Auwera GA, Carneiro MO, Hartl C, et al. From FastQ data to high confidence variant calls: the Genome Analysis Toolkit best practices pipeline. *Curr Protoc Bioinformatics*. 2013;43:11 10 11-11 10 33.
2. Cibulskis K, Lawrence MS, Carter SL, et al. Sensitive detection of somatic point mutations in impure and heterogeneous cancer samples. *Nat Biotechnol*. Mar 2013;31(3):213-219.
3. Koboldt DC, Zhang Q, Larson DE, et al. VarScan 2: somatic mutation and copy number alteration discovery in cancer by exome sequencing. *Genome Res*. Mar 2012;22(3):568-576.
4. Wang K, Li M, Hakonarson H. ANNOVAR: functional annotation of genetic variants from high-throughput sequencing data. *Nucleic Acids Res*. Sep 2010;38(16):e164.
5. Chen S, Zhou Y, Chen Y, Gu J. fastp: an ultra-fast all-in-one FASTQ preprocessor. *Bioinformatics*. Sep 1 2018;34(17):i884-i890.
6. Zhang Y, Park C, Bennett C, Thornton M, Kim D. Rapid and accurate alignment of nucleotide conversion sequencing reads with HISAT-3N. *Genome Res*. Jun 8 2021.
7. Langmead B, Trapnell C, Pop M, Salzberg SL. Ultrafast and memory-efficient alignment of short DNA sequences to the human genome. *Genome Biol*. 2009;10(3):R25.
8. Langmead B, Salzberg SL. Fast gapped-read alignment with Bowtie 2. *Nat Methods*. Mar 4 2012;9(4):357-359.
9. Dobin A, Davis CA, Schlesinger F, et al. STAR: ultrafast universal RNA-seq aligner. *Bioinformatics*. Jan 1 2013;29(1):15-21.
10. Kent WJ. BLAT--the BLAST-like alignment tool. *Genome Res*. Apr 2002;12(4):656-664.
11. Rodriguez-Perales S, Torres-Ruiz R, Suela J, et al. Truncated RUNX1 protein generated by a novel t(1;21)(p32;q22) chromosomal translocation impairs the proliferation and differentiation of human hematopoietic progenitors. *Oncogene*. Jan 7 2016;35(1):125-134.
12. Marin-Rubio JL, Perez-Gomez E, Fernandez-Piqueras J, Villa-Morales M. S194-P-FADD as a marker of aggressiveness and poor prognosis in human T-cell lymphoblastic lymphoma. *Carcinogenesis*. Oct 16 2019;40(10):1260-1268.
13. Livak KJ, Schmittgen TD. Analysis of relative gene expression data using real-time quantitative PCR and the 2(-Delta Delta C(T)) Method. *Methods*. Dec 2001;25(4):402-408.